Journal of Cellular Biochemistry Supplement 36:107–116 (2001)

Tacrolimus, but not Cyclosporine A, Significantly Increases Expression of ICAM-1 and IFN-γ in the NOD Mouse

Gianpaolo Papaccio,[1]* Michael V.G. Latronico,[2] Antonio Graziano,[1] Alessandro Lanza,[1] and Marcella Pedullà[3]

[1]Department of Experimental Medicine, Laboratory of Histology, School of Medicine, Second University of Naples, 80138 Naples, Italy
[2]I.N.M. Neuromed, Pozzilli (Isernia), Italy
[3]Department of Pediatrics, School of Medicine, Second University of Naples, 80138 Naples, Italy

Abstract We studied the alterations of cytokines and ICAM-1 expression in the NOD mouse pancreas produced by the administration of Cyclosporine A (CY) and Tacrolimus (TA), two widely used immunosuppressive drugs. Results evidenced differences in the effects of these two drugs. In fact, during treatment and after withdrawal, CY-treated animals remained euglycemic, showed good islet cell preservation and had low levels of Th1 and Th2 cytokines; ICAM-1 positivity within the islets was also found to be relatively low. On the other hand, TA-treated animals had infiltrated islets containing numerous dendritic cells, adhesion molecule overexpression, increased IFN-γ and ICAM-1 mRNA transcripts, and interestingly, high levels of circulating ICAM-1. However, even these animals remained euglycemic. These findings lead to the thought that these drugs may exert their effects in very different ways. Moreover, in TA-treated animals, the presence of an islet infiltrate containing numerous dendritic cells coupled with maintenance of euglycemia is suggestive for the involvement of immunosurveillance mechanisms. J. Cell. Biochem. Suppl. 36:107–116, 2001.

Key words: immunosuppression; cytokines; adhesion molecules; NOD mice

Type 1 diabetes is an autoimmune disease associated with selective destruction of pancreatic islet β cells. In the nonobese diabetic (NOD) mouse, infiltration by mononuclear cells, especially during the early stages of the disease, involves not only the islets but also the whole pancreas and its ducts in particular [Papaccio et al., 1993]. This early stage of infiltration is characterized by Th2 rather Th1 infiltrating cells [Shehadeh et al., 1993; Muir et al., 1995].

Immunocytochemical studies performed in these animals demonstrate that infiltrating cells within and around islets and ducts express Ia-b (class II) molecules [Papaccio et al., 1991; Linn et al., 1994]. In addition, an increased expression of adhesion molecules, which serve to bind mononucleates, has been described in the human pancreas [Hänninen et al., 1992]. Furthermore, MHC class II and Intercellular Adhesion Molecule 1 (ICAM-1) immunoreactivities have been reported in extra-islet structures, such as pancreatic endothelial cells [Linn et al., 1994] and pancreatic ducts [Papaccio et al., 1994a] in the NOD mouse. Also, endothelial cells of both peri-islet and extra-islet compartments often show Ia-b and ICAM-1 immunoreactivities, demonstrating that these molecules are important for the adhesion processes taking place during early autoimmune inflammation [Papaccio et al., 1998]. It has also been shown that islet β cells adjacent to infiltrating lympho-

Grant sponsor: MURST (Italian Ministry for Research and University); Grant number: PRIN 99; Grant sponsor: Second University of Naples; Grant number: Campania Region, L-R. no. 41/94.

*Correspondence to: Gianpaolo Papaccio, Department of Experimental Medicine, Laboratory of Histology, Second University of Naples, via L. Armanni, 5, 80138 Naples, Italy. E-mail: gianpaolo.papaccio@unina2.it

Received 18 September 2000; Accepted 6 November 2000

This article published online in Wiley InterScience, March 19, 2001.

cytes are stained by anti-ICAM-1 monoclonal antibodies and cytokines, secreted by islet-infiltrating mononuclear cells, can induce ICAM-1 expression on islet β cells [Yagi et al., 1995]. This mechanism has been hypothesized to be responsible for acceleration of β cell destruction by cytotoxic-T lymphocytes. These authors also suggest that immunointervention on the ICAM1/LFA-1 pathway would be an excellent strategy to prevent the disease [Yagi et al., 1995].

Up to now several studies have been devoted to the understanding of the pathophysiology of both Cyclosporine A (CY) and Tacrolimus (TA) and of their side effects on pancreatic islets; to our knowledge, studies have not been focused on their long-lasting effects and on their possible influence upon adhesion molecule expression. Moreover, only a few papers have described the effects of these immunosuppressants on cytokines, focusing mainly on TNF-α [Baquerizo et al., 1989; Takaori et al., 1992; Burke et al., 1994] and on IL-2 and IFN-γ [Asano et al., 1996]; in particular, it was demonstrated that IL-2 and IFN-γ expressions could be suppressed only for a limited period (5 days) by repeated high doses of TA.

Moreover, it has been shown that some cytokines, and particularly IFN-γ which is known to be a proinflammatory Th1 cytokine, are capable of inducing MHC class I and ICAM-1 expression [Chakrabarti et al., 1996]. Interestingly, it has been recently reported that soluble ICAM-1 (sICAM-1) is significantly enhanced during chronic autoimmune inflammation [Uchio et al., 1999]. Furthermore, IFN-γ exerts unexpected antidiabetogenic effects in diabetes-prone bio-breeding rats [Nicoletti et al., 1998].

Therefore, the purpose of this study was to investigate the effects of CY and TA on the expression of cytokines and ICAM-1 in the NOD mouse pancreas. Our results demonstrate that both drugs are capable of keeping blood glucose levels low in these spontaneously diabetic animals, but differently from CY, TA significantly enhances ICAM-1 expression and IFN-γ mRNA levels; however, it did not inhibit peri-islet infiltration in which numerous CD4 positive and dendritic cells could be detected. Furthermore, high sICAM-1 values were also observed. These findings suggest that TA acts upon the immune system involving immunosurveillance mechanisms.

MATERIALS AND METHODS

Animals

Six-week-old female NOD mice (Bommice, Bomholtgarten, Denmark) (n = 48) were used in the experiment. In this colony, clinically evident diabetes is observable by weeks 20–22 in 90–100% of females, but in less than 20% of males. The initial histopathological lesion is a perivasculitis seen by Week 5. Peri-insulitis and peri-ductulitis are present by Week 8 and insulitis is massive by Week 15. The animals, free from viral or bacterial infections and weighing 20–28 g, were checked weekly for non-fasting glycemia and were not subjected to insulin treatment.

Immunosuppression

CY (Sandimmun, Pharmacia, Italy) and TA (FK506, Fujisawa Pharmaceutical, London, UK) were used for immunosuppression. Animals were immunosuppressed either with CY (n = 16) dissolved in distilled water and used at a concentration of 1.8 mg/mouse/week, or with TA (n = 16) suspended in distilled water and given at a dose of 5 mg/kg b. wt. orally in a volume of 3 ml/kg once a day. The dose of both drugs (CY and TA) corresponds to the therapeutic dose previously used by us and other researchers for immunosuppression of type 1 diabetes in rodent animal models [Papaccio et al., 1989, 1994b; Hirano et al., 1992]. Control NOD animals (n = 16) were treated with physiologic saline (five times per week).

Treatment was initiated at the age of 6 weeks and continued for 10 weeks. At Weeks 10 (n = 8), 20 (n = 8), and 25 (n = 8), animals were anaesthetized with ether and the pancreas removed for morphological evaluations.

Glycemia

Blood glucose levels were tested weekly using the hexokinase method (Boehringer, Mannheim, Germany). Animals were considered hyperglycemic when their non-fasting blood glucose levels were higher than 8 mM/l, but lower than 12 mM/l on two successive determinations. Mice were considered diabetic when their blood glucose levels exceeded 12 mM/l.

Circulating ICAM-1

Soluble ICAM-1 activity was assayed using the ELISA CD54 kit (Endogen, Woburn, MA). Blood samples from each animal were collected

from the retro-orbital plexus and processed following the kit's instructions. Values are expressed as ng/ml.

Standard Light Microscopy and Assessment of Insulitis Severity

Pancreatic samples from each animal were fixed with Bouin's fixative and embedded in paraffin. Specimens were sectioned serially (5 μm thick) and stained with hematoxylin eosin or Gomori aldehyde fuchsin for general morphology and for the evaluation of islet and extra-islet infiltration. The severity of insulitis was assessed and scored as follows: 0, no infiltration; 1, peri-insulitis; 2, peri-insulitis with single leukocyte invading the islet parenchyma; 3, $<50\%$ intraislet infiltration; 4, invasive insulitis ($>50\%$); 5, complete infiltration (up to 100%); 5, islet atrophy and retraction due to islet β cell loss. For each section, scores were summed and divided by the total number of islets scored to obtain an average.

Immunocytochemistry

Samples from the tail of each pancreas were collected and kept frozen in liquid nitrogen. Randomly selected cryocut sections were stained by indirect avidin-biotin peroxidase as previously described [Papaccio et al., 1991]. The monoclonal antibodies used were: anti(MHC class II (IgG_1; Dakopatts, Milan, Italy); anti-ICAM-1 (clone CD45; Dakopatts); anti-T lymphocyte antibodies (Dakopatts) including CD4 (MT310) and CD8 (DK24); anti-macrophage antibody EBM-11 (Dakopatts); anti-dendritic cells (MIDC-8, BMDA, Augst, Switzerland), anti-insulin, anti-glucagon, and anti-somatostatin antibodies (Dakopatts). The secondary antibody was biotinylated goat anti-mouse antibody. As a negative control, the primary antibody was replaced with goat non-immune serum. The other antibodies were used to distinguish infiltrating cells, and to detect any insulin-, glucagon- or somatostatin-secreting cells lining the pancreatic ducts, as well as to observe the presence of residual insulin-containing β cells in the islets of 20- or 25-week-old NOD mice.

Sections of 5 μm thickness were examined for semiquantitative analysis. The immunoreactive cells on alternate sections were determined at a magnification of $\times 400$ using an eyepiece with a square-ruled grid with a total area of 0.062 mm^2 and counted utilizing the M4 image analysis system (Imaging Brock University, St. Catherines, Ontario, Canada) in 60 different areas. This allowed the calculation of immunoreactive cells/$mm^2 \pm$ SEM. The observations were carried out blindly by three different researchers.

Ultrastructure

For transmission electron microscopy (TEM), samples were cut into small cubes and immediately fixed in 0.1M phosphate-buffered solution of 2.5% glutaraldehyde (pH 7.4) for 2 h at 4°C, then washed and postfixed in 1% OsO_4 in the same buffer for 1 h at 4°C. Specimens then were dehydrated, embedded in epoxy-resins and sectioned on an ultratome (Reichert Ultracut E, Germany). The first 10 islets and ducts encountered in the semithin sections of the pancreas of each animal were examined and screened for ultrathin sectioning. Uranyl acetate and lead citrate stained ultrathin sections were examined under the electron microscope (Zeiss EM 109, Germany).

Islet Leukocyte Preparations

Pancreatic islets were isolated by collagenase digestion and purified on a Ficoll density gradient. Single cells were dispersed from handpicked islets by incubation at 37°C for 10 min in Ca^{2+}/Mg^{2+}-free PBS containing 0.2mg/ml EDTA, followed by injection through progressively narrower gauge needles. Mononuclear leukocytes were separated from other cells by density gradient centrifugation on Percoll.

Semiquantitative Cytokine mRNA Determination

RNA was extracted from islet leukocytes of each animal using the guanidinium thiocyanate method [Chirgwin et al., 1979], modified as follows: cells were homogenized in 4 M/l guanidinium thiocyanate solution containing 17 mM/l sodium *N*-lauroylsarcosine, 25 mM/l sodium citrate, 0.1 M/l 2-ME, and 0.1% Antifoam A, 30% aqueous emulsion (Sigma, Milan, Italy), then precipitated with ethanol, pelleted, and re-extracted with 8 M/l guanidine hydrochloride:0.5 M/l EDTA (19:1). After pelleting and drying, samples were extracted twice with phenol:chloroform (1:1) and precipitated with ethanol. cDNA synthesis was carried out on total RNA from each animal with Superscript reverse transcriptase kit (Life Technologies, Gibco BRL, Milan, Italy) by using oligo $(dt)_{12-18}$ and Moloney murine leukemia virus reverse transcriptase (20 U) in a 25 μl reaction at 37°C

TABLE I. Oligonucleotide Primer Sequences Used in the PCR Amplification

Gene	5′ primer	3′ primer
II-2	CAAAGGAAACACAGCAGCACCTGG	TCCTCAGAAATTCCACCACAGTTGC
IL-4	GTCACTGACTGTAGAGAGCTATT	AGGTACATCACGTGGGAAGTAAA
TNF-α	TACTGAACTTCGGGGTGATTGGTCC	CAGCCTTGTCCCTTGAAGAGAACC
IFN-γ	ATCTGGAGGAACTGGCAAAAGGACG	CCTTAGGCTAGATTCTGGTGACAGC
ICAM-1	ACCTGCGGCCCCAAGGGCTG	CTCTAGGACCCGGGGGCTGA
Cyclophilin	GACAGCAGAAAACTTTCGTGC	TCCAGCCACTCAGTCTTGG

for 1.5 h. The reverse transcriptase reaction containing cDNA was diluted 1:30, 1:90, and 1:270 in sterile H_2O. Polymerase chain reaction (PCR) amplification was carried out on the cDNA from each animal using 3 μl of each dilution of cDNA in a 20 μl reaction with 80 ng of each primer, 0.25 mM/l of each dNTP, 2.5 μCi of [α- ^{32}P] dCTP (3,000 Ci/mM; DuPont-NEN, Milan, Italy), 1U of AmpliTaq (Perkin-Elmer/Cetus, Monza, Italy), and 3 mM/l Mg^{2+}. The oligonucleotide primer sequences used in the PCR amplification are shown in Table I. Samples were amplified through 40 cycles at 94°C for 20 s, 60°C for 20 s, and 72°C for 30 s in a Gene Amp PCR System 9600 (Perkin-Elmer/Cetus Monza, Italy). The PCR reaction was electrophoresed on 1.5% agarose gels, transferred to nylon membranes, and ^{32}P incorporation in cytokine and cyclophilin DNA bands was determined by phosphoimager analysis for each cytokine (TNF-α, IL-2, IL-4, IFN-γ) and ICAM-1. PCR products were normalized as a percentage of ^{32}P incorporated in cyclophilin PCR product amplified from the same cDNA preparation. In these experiments, the template used for PCR amplification was cDNA from NOD splenocytes activated with concavalin A for 3 days to express the different cytokine messages. This cDNA also was used as a positive control in all PCR runs. Under the conditions used, the PCR product signal was proportional to the amount of RNA/cDNA subjected to PCR amplification. All PCR products compared were produced in the same PCR run.

Statistical Evaluation

Student's *t*-test and analysis of variance (ANOVA) were used for statistical analysis. The level of significance was set at $P < 0.05$.

RESULTS

Immunosuppressed NOD Animals are Euglycemic

Figure 1 shows blood glucose values in control and immunosuppressed animals. Untreated 10-week-old NOD mice were normoglycemic. Twenty-week-old animals were clearly diabetic ($P < 0.0001$ vs. CY- and TA-treated animals), and by 25 weeks these animals were overtly diabetic. CY-treated and TA-treated animals remained normoglycemic throughout the experiment ($P < 0.0001$ vs. age matched untreated NOD).

Tacrolimus-Immunosuppressed Animal Islets Remain Infiltrated During Treatment

Untreated 10-week-old NOD mice showed peri-islet infiltration surrounding the majority of the islets. By 20 weeks these animals had either extensively infiltrated islets by mononuclear leukocytes (intra-islet insulitis) or islets of small dimensions (atrophic or retracted with evident signs of cytoarchitectural derangement).

CY-immunosuppressed animals of the same ages (10- and 20-weeks-old) showed no signs of

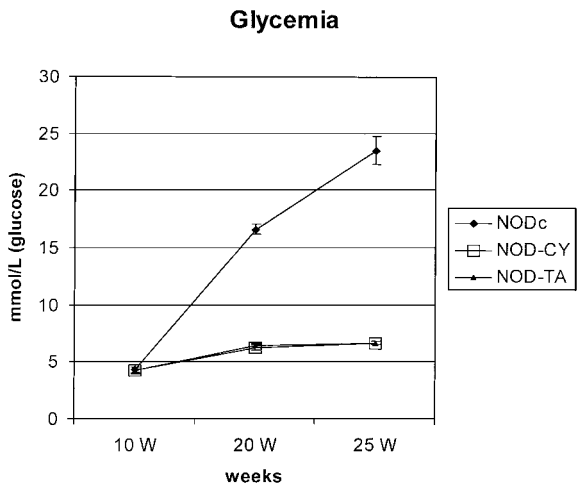

Fig. 1. Figure showing blood glucose levels in control and immunosuppressed NOD animals (n=48). Values, given as mM/l glucose, are expressed as means ±SD. (Blood glucose range in control nondiabetic animals = 4.5 to 5.5 mM/l). It is clearly shown that CY-(n=16) and TA-treated (n=16) animals had significantly lower blood glucose levels ($P < 0.0001$), when compared to untreated controls at Weeks 20 and 25.

TABLE II. Insulitis Grading Score in NOD Controls (NODc), Immunosuppressed NOD With Cyclosporine A (NODi CY) or Immunosuppressed NOD With Tacrolimus (NODi TA)

	Week 10	Week 20	Week 25
NODc	1.0 ± 0.2	$3.5 \pm 0.3^{*}$	$4.2 \pm 0.4^{*}$
NODi (CY)	0.2 ± 0.1	0.2 ± 0.1	0.2 ± 0.1
NODi (TA)	1.0 ± 0.2	$2.0 \pm 0.6^{**}$	$2.3 \pm 0.6^{**}$

Data are given as means $\pm$SD.
*$P<0.001$ vs. all groups; **$P<0.01$ vs. NODi (TA) week 10 and vs. NODi (CY) all weeks.

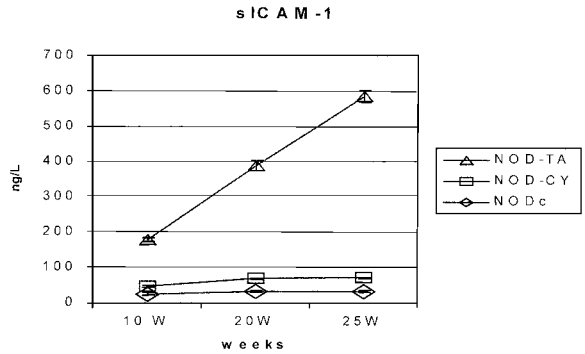

Fig. 2. Figure showing circulating Intercellular Adhesion Molecule-1 (sICAM-1) levels. sICAM-1 values, expressed as ng/l are means $\pm$ SD. (Control animal range=11–100 ng/l). The figure shows that TA-treated animal (n=16) levels are significantly increased ($P < 0.0001$), with respect to control and CY-treated NOD mice. Levels of sICAM-1 in TA-treated mice are also significantly increased with the age ($P < 0.0001$).

insulitis or islet atrophy, and islet cytoarchitecture was preserved (Table II). On the other hand, 10-week-old TA-treated animals showed peri-islet infiltration which worsened by week 20 ($P<0.01$ for scores at Week 10 vs. Week 20).

At Week 25, nine weeks after treatment withdrawal, CY-treated animals still did not show signs of islet infiltration while TA-treated animals continued to show clear peri-islet infiltration with single invading leukocytes. Untreated NOD mice islets were atrophied with islet β cells loss and contained infiltrating leukocytes.

Tacrolimus Dramatically Enhances Soluble ICAM-1

Figure 2 shows sICAM-1 levels found in control and immunosuppressed animals. Circulating ICAM-1 values were dramatically en hanced in TA-treated animals with respect to control and CY-treated NOD mice ($P < 0.0001$). Moreover, levels significantly increased with the age of TA-treated mice ($P < 0.0001$).

Tacrolimus Significantly Enhances ICAM-1 Molecule Expression

Pancreas from untreated 10-week-old animals did not show MHC class II immunoreactivity. However, there was low ICAM-1 positivity (see Table III for semiquantitative evaluation). At 20 weeks, these animals started to show MHC class II immunoreactivity, limited to the connective layer surrounding ducts and ICAM-1 expression increased (Fig. 3). The latter was considerably greater than that of MHC class II molecules of pancreas belonging to animals of the same age ($P < 0.001$). An intense immunoreactivity was observed particularly at the level of ducts, including the epithelial lining, endothelia, and some islet and pancreatic cells along septa. Islets had a normal pattern for glucagon and somatostatin but only rare insulin-positive cells. CD8 or EBM-11 immunoreactivities were not observed on ducts or in islets, but a few CD4 immunoreactive cells were seen.

Immunosuppressed animals at Weeks 10 and 20 also expressed ICAM-1 structures at the islet, duct, and endothelial levels; in particular, TA treatment enhanced ICAM-1 immunoreactivity already by Week 10, and further increased expression by Week 20 with respect to that seen in control diabetic animals (Fig. 4). CY treatment produced lower adhesion molecule expression (Fig. 5) with respect to that observed in control and TA-treated animals (see Table III). MHC class II structures were rarely observed. CD4 positive cells were observed at the islet periphery but only in TA-treated animals, in which numerous MIDC-8 immunoreactive cells (dendritic cells) were also seen (Fig. 6).

Differences between CY-treated and TA-treated animals were enhanced at Week 25; in fact, while CY did not particularly alter ICAM-1 positivity further, TA-treated animals showed a significantly higher expression of this molecule ($P < 0.001$).

Ultrastructure

In untreated NOD, infiltrating cells were observed jammed between epithelial cells of pancreatic ducts or in the connective layer in diabetic animals at the ultrastructural level. Epithelial cells showed no signs of alteration and there was no expansion of the ductal epithelium. At Week 25, islets were of small dimensions and rare degranulated islet-β cells

TABLE III. Semiquantitative Evaluation of Immunoreactive Cells in Islets, Ducts, and Endothelia of NOD Control (NODc) and Immunosuppressed NOD (NODi) (CY=Cyclosporine A) (TA=Tacrolimus) Animals

Antibody	Strain	Week 10	Week 20	Week 25
MHC classII	NODc	1.0 ± 0.2	2.0 ± 0.5	1.5 ± 0.5
	NODi (CY)	1.0 ± 0.2	1.0 ± 0.2	1.5 ± 0.2
	NODi (TA)	1.0 ± 0.2	1.5 ± 0.2	2.0 ± 0.2
ICAM-1	NODc	4.0 ± 1.5	$10.5 \pm 1.0^{*1}$	10.0 ± 1.5
	NODi (CY)	3.5 ± 1.0	$7.2 \pm 2.0^{*}$	6.5 ± 2.0
	NODi (TA)	10.2 ± 2.0^{2}	12.0 ± 2.5	$15.5 \pm 2.5^{**}$
CD4	NODc	1.0 ± 0.2	3.0 ± 0.5	1.0 ± 0.2
	NODi (CY)	1.0 ± 0.2	1.0 ± 0.2	1.5 ± 1.0
	NODi (TA)	2.0 ± 0.5	$4.5 \pm 1.0^{**}$	$4.5 \pm 1.5^{**}$
CD8	NODc	0.5 ± 0.2	1.5 ± 0.5	1.0 ± 0.2
	NODi (CY)	1.0 ± 0.2	1.0 ± 0.1	1.0 ± 0.2
	NODi (TA)	1.5 ± 0.4	1.5 ± 0.2	2.0 ± 0.2
EBM-11	NODc	0.5 ± 0.2	1.0 ± 0.2	0.2 ± 0.1
	NODi (CY)	0.2 ± 0.1	0.2 ± 0.1	0.2 ± 0.1
	NODi (TA)	1.0 ± 0.2	1.0 ± 0.2	$2.5 \pm 1.0^{**}$
MIDC-8	NODc	2.2 ± 0.6	0.5 ± 0.2	0.2 ± 0.1
	MODi (CY)	2.0 ± 0.5	0.6 ± 0.2	0.2 ± 0.1
	NODi (TA)	3.0 ± 0.6	$5.6 \pm 0.2^{***}$	$5.8 \pm 0.1^{***}$

The immunoreactive cells on alternate sections were determined at a magnification of ×400 using an eyepiece with a square-ruled grid with a total area of 0.062 mm^2 and counted with M4 image analysis system (Imaging-Brock University, St. Catherin, Ontario, Canada) in 60 different areas. This allowed the calculation of immunoreactive cells/mm^2 ± SEM. The observations were carried out blindly by three different researchers $^{*}P < 0.001$ vs. MHC class II immunoreactive cells in all animal groups; $^{**}P < 0.001$ vs. 25-week old NODc and NODi-CY treated; $^{***}P < 0.001$ vs. MIDC-8 week 10 and $P < 0.0001$ vs. NODc and NODi-CY; $^{1}P < 0.05$ vs. ICAM-1 of NOD-CY immunosuppressed animals; $^{2}P < 0.001$ vs. ICAM-1 week 10 other groups.

or non-β cells, often still surrounded by infiltrating leukocytes, were observed.

At Weeks 10 or 20 immunosuppressed animal islets were either normal or showed a peri-islet infiltration. Dendritic cells often were found in TA-treated animals (Fig. 7). Occasionally, monocyte or lymphocyte margination and trapping within islet and in peri-islet capillaries, was observed (Fig. 8). Endothelial cells were hypertrophic, had numerous cytoplasmic protrusions and increased pinocytotic vesicles. Several were separated by deep gaps. There were no ultrastructural alterations of ducts.

At Week 25, infiltrated cells were observed surrounding islets and ducts and filling peri-islet capillaries of TA-treated animals.

Cyclosporine A Decreases Cytokine Production but Tacrolimus Significantly Increases IFN-γ and ICAM-1 Transcripts

Cytokine mRNA levels in mononuclear leukocytes isolated from islets of untreated and immunosuppressed animals are shown in Figure 9.

The purity of mononuclear leukocytes separated from islets of untreated and immunosuppressed NOD ranged from 70 to 82%.

We analyzed the expression of IL-2, IL-4, IFN-γ and TNF-α, in order to determine the cytokine profiles of islet infiltrating T lymphocytes. The level of each of these cytokines was low in 10-week-old animals but increased in 20-week-old NOD controls. At this point of time, IFN-γ expression in TA-treated animal islets was significantly greater than in age-matched CY immunosuppressed NOD ($P < 0.001$). At Week 25, transcripts continued to increase in TA-treated animal islets while CY-treated animals still had low levels (TA vs. CY, $P < 0.001$); IFN-γ transcripts were also significantly higher with respect to those found in control NOD animals ($P < 0.001$). To determine whether the increase in ICAM-1 protein is accompanied by an increase in the corresponding mRNA, we also measured the level of ICAM-1 mRNAs. Interestingly, ICAM-1 mRNA transcripts were increased in TA-immunosuppressed animals already by week 10 ($P < 0.001$). IL-4 was found to be very low in all cases.

DISCUSSION

This study evidences that CY and TA are both capable of counteracting hyperglycemia by preserving islet cells of NOD mice from destruction even after treatment withdrawal. It also

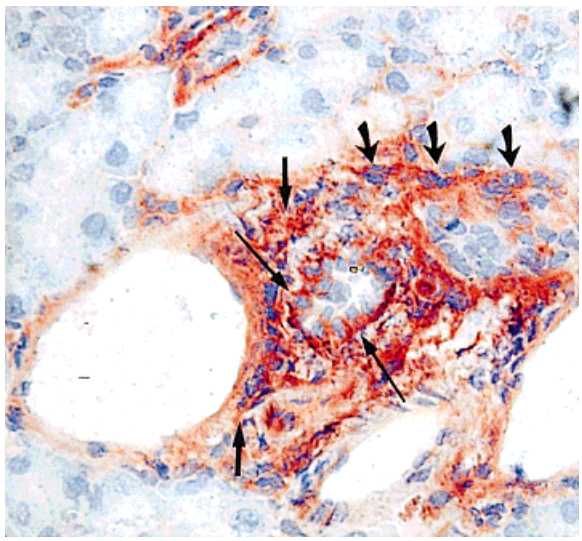

Fig. 3. Light micrograph of a 20-week-old diabetic NOD control mouse pancreas showing ICAM-1 immunoreactive structures, located both at the level of the connective (thick arrows) and epithelial layers (arrows) of a duct. ICAM-1 immunoreactivity involves the whole epithelial layer. Several islet cells (curved arrows) are also ICAM-1 immunoreactive. (Original magnification × 300).

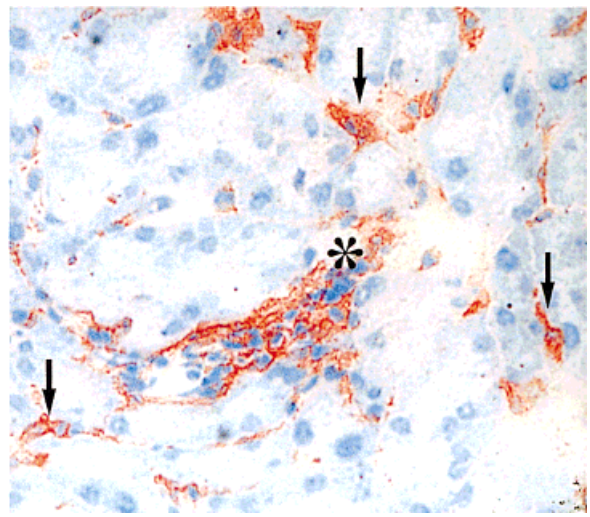

Fig. 5. Light micrograph of a pancreas from a 20-week-old NOD mouse immunosuppressed with Cyclosporine A, showing ICAM-1-immunoreactive cells near endocrine cell clusters (asterisk) and along septa in the exocrine tissue (arrows). (Original magnification × 300.)

shows that, while CY maintains both euglycemia and islet cell preservation by counteracting islet infiltration and by lowering Th1 cytokine and ICAM-1 levels, TA does not inhibit the formation of an islet infiltrate containing numerous dendritic cells; adhesion molecule overexpression, an increase in ICAM-1 mRNA transcripts and an increase in IFN-γ are also seen. Particularly interesting is also the finding that TA increases circulating ICAM-1 levels.

The role played by different cytokines in type 1 diabetes is now under considerable revision, mainly in the light of recent studies, which demonstrate that Th1 cytokines such as IFN-γ

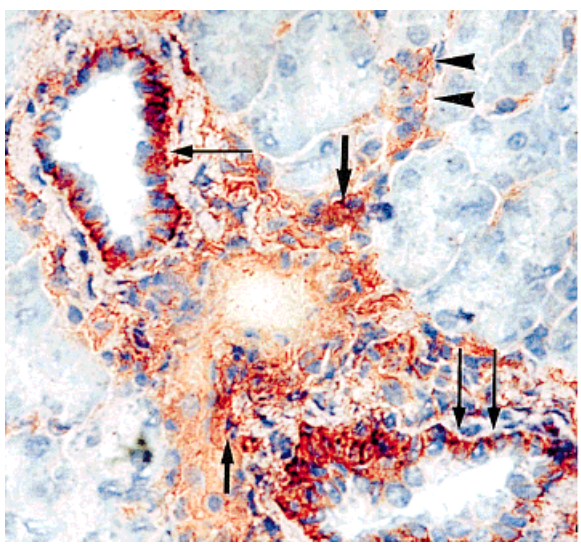

Fig. 4. Light micrograph of a pancreas from a 20-week-old NOD mouse immunosuppressed with Tacrolimus, showing ICAM-1-immunoreactive cells (arrows) of a duct. ICAM-1 immunoreactivity is also observable at the level of the connective layer (thick arrows) as well as on cells along septa (arrowheads). (Original magnification × 300.)

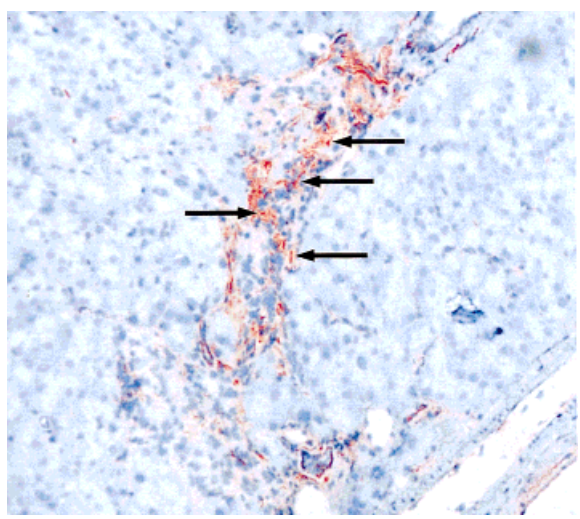

Fig. 6. Micrograph of a pancreas from a 25-week-old NOD mouse immunosuppressed with Tacrolimus, showing numerous MIDC-8 (dendritic cells) around and within an islet (arrows). (Original magnification × 100.)

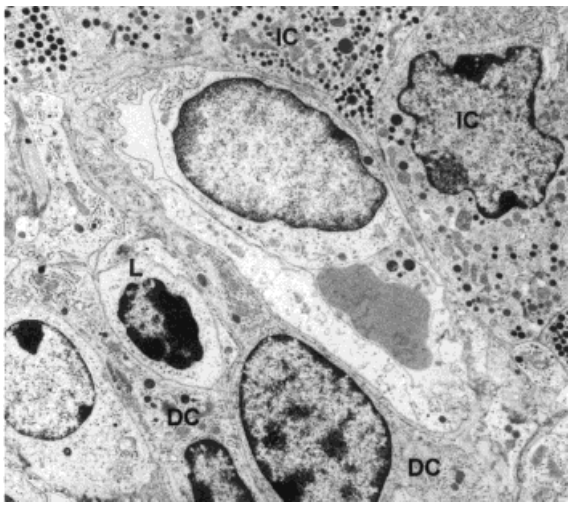

Fig. 7. Transmission electron micrograph from a 20-week-old NOD mouse immunosuppressed with Tacrolimus showing dendritic cells (DC) and a lymphocyte (L) in the peri-islet infiltrate. (IC=islet cell; Original magnification × 4.500.)

[Nicoletti et al., 1998] and IL-18 (interferon-gamma inducing factor) [Rothe et al., 1998], paradoxically suppress diabetes development probably by locally downregulating Th1 cytokine expression or β cell toxic mediators. This new information could stimulate further debate on this topic and could lead to a rethinking of recent data on the specific role of the various cytokines. The other anti-inflammatory effects

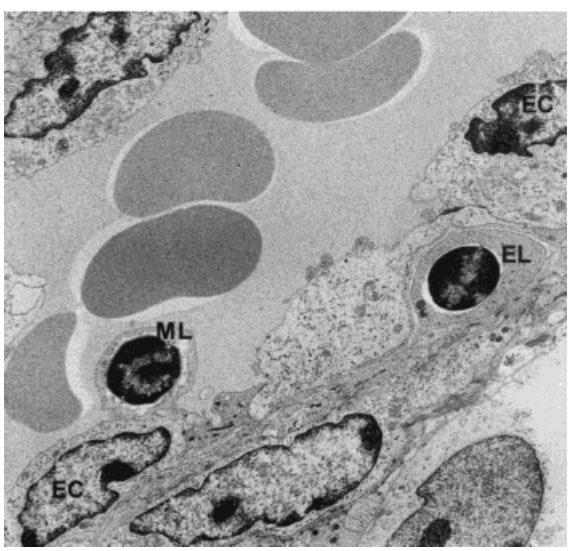

Fig. 8. Transmission electron micrograph from a 20-week-old NOD mouse immunosuppressed with Tacrolimus showing a marginating lymphocyte (ML), an emigrating lymphocyte (EL) and hypertrophic endothelial cells (EC). (Original magnification × 4.500.)

of IFN-γ include: (i) reduction of IL-1β production/action by inhibiting IL-1β secretion and upregulating IL-1β receptor agonist production [Landolfo and Garotta, 1991]; (ii) downregulation of monocyte chemotaxis through diminished expression of C3a [Wahl et al., 1991]; and (iii) induction of CD8 suppressor T cells [Balashov et al., 1995]. Th1 and Th2 cytokines are not produced exclusively by Th1 and Th2 cells (subsets of $CD4^+$ cells). They are also produced by other immune cell types such as $CD8^+$ T-cells, macrophages, NK cells, and B cells [Fitch et al., 1993; Seder and Paul, 1994; Suarez-Pinzon et al., 1996]. However, the final effector mechanism by which Th1 promoting cytokines leads to islet β cell destruction remains unknown.

In this study the higher levels of IFN-γ found in TA- immunosuppressed animals with respect to CY-treated mice are not correlated with greater severity of pancreatic inflammation, but only with peri-islet infiltration and with increased levels of ICAM-1 (circulating, mRNAs and immunoreactivity); therefore, a rather intriguing role for IFN-γ comes out from this report; i.e., a possible and suggestive influence of this cytokine upon adhesion molecules and ICAM-1 in particular. This high level of circulating ICAM-1 may be responsible for the inhibition of LFA-1 mediated adhesiveness on lymphocytes aiding immunosuppressive activity. This is also strongly suggested by the finding that chronic autoimmune inflammation is maintained through high sICAM-1 levels [Uchio et al., 1999].

These interesting observations must be taken into consideration for many reasons. Up to now the role of these adhesion molecules as well as other integrins in type 1 diabetes has not been well defined. In general, these adhesion molecules are thought to specify cell–cell interactions in embryogenesis and histogenesis. ICAM-1 induction by autoimmune mechanisms which take place in type 1 diabetes, and its persistence in pancreatic ducts, islets, and endothelia of overtly diabetic animals, confirm that a role for ICAM-1 is not only to facilitate interactions between cells involved in adherence and emigration processes, but also to mediate interactions between cells of the immune and endocrine systems [Springer, 1990].

In addition, the observation of trapped monocytes and of hypertrophic endothelial cells

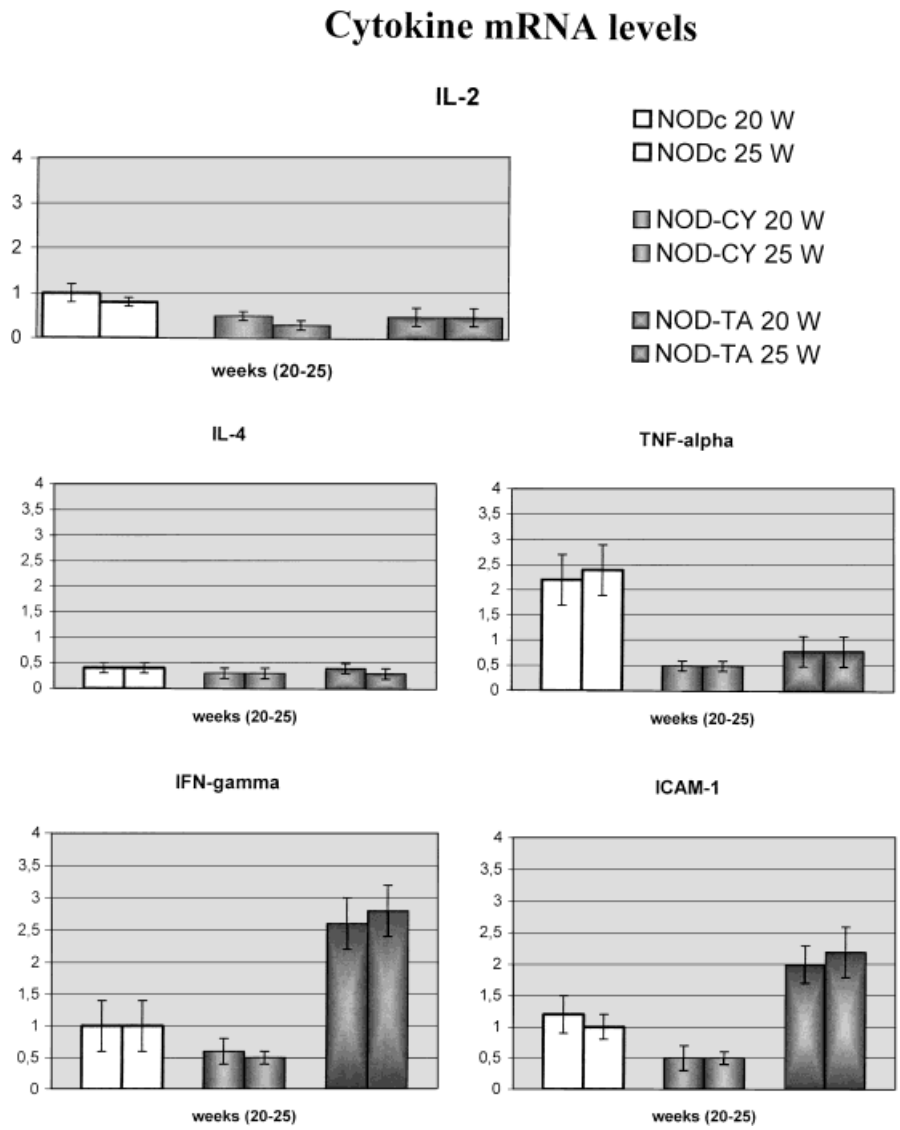

Fig. 9. Cytokine mRNA levels in leukocytes from isolated islets of untreated and immunosuppressed NOD mice. Cytokine mRNA levels (PCR product) are expressed as a percentage of the cyclophilin PCR product amplified from the same cDNA preparation. Cytokine mRNA levels (mean SE) are shown for each group of mice. The figure shows that IFN-γ mRNA transcripts of TA-treated animals are significantly higher when compared to those found in control and CY-treated mice, mainly at week 25 ($P < 0.001$). Also ICAM-1 mRNA transcripts were found to be significantly higher in TA-treated animals when compared to controls and CY-treated mice ($P < 0.001$).

within the islets, previously described in prediabetic NOD mice [Papaccio et al., 1998], stresses that the processes leading to diapedesis, still observable in TA-immunosuppressed animals, could itself be seen as part of an immune response in which the immune system is under continuous stimulation. This is of some significance for long-lasting immunosurveillance and suggests that infiltration may occur because of the persistence of such autoimmune stimuli.

Therefore, the effect of TA upon pancreatic islets is different from that of CY in that it also involves immunosurveillance by dendritic cells, and an increase of IFN-γ and ICAM-1 which may cooperate to maintain the morphology and function of islet β cells.

In conclusion, this study demonstrates that TA but not CY: (1) significantly enhances IFN-γ levels; (2) considerably increases ICAM-1 proteins and their mRNA transcripts, as well as circulating ICAM-1; and (3) maintains euglyce-

mia in the presence of an islet infiltrate that contains numerous dendritic cells.

ACKNOWLEDGMENTS

This work was supported with MURST (Italian Ministry for Research and University) (PRIN 99), Second University of Naples Grant and Regional Funds (Campania Region, L.R. no. 41/94) (G.P.).

REFERENCES

Asano K, Taki M, Matsuo S, Yamada K. 1996. Mode of action of FK-506 on protective immunity to Hymenolepis nana in mice. In Vivo 10:537–545.

Balashov KE, Khoury SJ, Hafler DA, Weiner HL. 1995. Inhibition of T cell responses by activated human $CD8^+$ T cells is mediated by interferon-gamma and is defective in chronic progressive multiple sclerosis. J Clin Invest 95:2711–2719.

Baquerizo H, Leone J, Pukel C, Wood P, Rabinovitch A. 1989. Mechanisms of cyclosporine protection against spontaneous diabetes mellitus in the BB/W rat. J Autoimmunity 2:133–150.

Burke GW, Cirocco R, Marokou M, Agramone RF, Rabinovitch A, Miller J, Skyler JS. 1994. Effect of cyclosporine A on serum tumor necrosis factor alpha in new-onset type 1 (insulin-dependent) diabetes mellitus. J Diabetes Complic 8:40–44.

Chakrabarti D, Huang X, Beck J, Henrich J, McFarland N, James RFL, Stewart TA. 1996. Control of islet intercellular adhesion molecule-1 expression by interferon-α and hypoxia. Diabetes 45:1336–1343.

Chirgwin JM, Przybyla AE, MacDonald RJ, Rutter KT. 1979. Isolation of biologically active ribonucleic acid from sources enriched in ribonuclease. Biochemistry 18:5294–5299.

Fitch FW, McKisic MD, Lancki DW, Gajewski TF. 1993. Differential regulation of murine T lymphocyte subsets. Ann Rev Immunol 11:29–48.

Hänninen A, Jalkanen S, Salmi M, Toikkanen S, Nikilakros G, Simell O. 1992. Macrophages, T cell receptor usage and endothelial cell activation in the pancreas at the onset of insulin-dependent diabetes mellitus. J Clin Invest 90:1901–1910.

Hirano Y, Fujihira S, Ohara K, Katsuki S, Noguchi H. 1992. Morphological and functional changes of islets of Langerhans in FK506-treated rats. Transplantation 53:889–894.

Landolfo S, Garotta G. 1991. IFN-λ: an immunomodulatory and proinflammatory lymphokine. J Immunol Res 9:81–94.

Linn T, Strate C, Federlin K, Papaccio G. 1994. Intercellular-adhesion-molecule-1 (ICAM-1) expression in the islets of nonobese diabetic (NOD) and low-dose streptozocin-treated mouse pancreas. Histochemistry 97:371–374.

Muir A, Peck A, Clare-Salzler M, Song Y-H, Cornelius J, Luchetta R, Krischer J, Maclaren N. 1995. Insulin immunization of NOD mice induces a protective insulitis characterized by diminished intraislet interferon γ-transcription. J Clin Invest 95:628–634.

Nicoletti F, Zaccone P, Di Marco R, Magro G, Grasso S, Stivala F, Calori G, Mughini L, Meroni PL, Garotta G. 1998. Paradoxical antidiabetogenic effect of γ-interferon in DP-BB rats. Diabetes 47:32–38.

Papaccio G, Esposito V, Mezzogiorno V. 1989. Recovery from pancreatic side effects after the withdrawal of cyclosporine A treatment in bio breeding and Wistar rats. Micron and Micr Acta 20:88–97.

Papaccio G, Linn T, Federlin K, Volkmann A, Esposito V, Mezzogiorno V. 1991. Further morphological and biochemical observations on early low dose streptozocin diabetes in mice. Pancreas 6:659–667.

Papaccio G, Chieffi Baccari G, Mezzogiorno V, Esposito V. 1993. Extraislet infiltration in NOD mouse pancreas: observations after immunomodulation. Pancreas 8:459–464.

Papaccio G, Chieffi Baccari G, Strate C, Linn T. 1994a. Pancreatic duct inflammatory infiltration in the nonobese diabetic (NOD) mouse. J Anat 185:465–470.

Papaccio G, Esposito V, Chieffi Baccari G. 1994b. The immunosuppressant FK506 inhibits the damage to mouse pancreatic islets induced by low dose streptozocin. Cell Tissue Res 277:573–578.

Papaccio G, Latronico MVG, Pisanti FA, Federlin K, Linn T. 1998. Adhesion molecules and microvascular changes in the nonobese diabetic (NOD) mouse pancreas. An NO-inhibitor (L-NAME) is unable to block adhesion inflammation-induced activation. Autoimmunity 27:65–77.

Rothe H, Hausmann A, Casteels K, Mathieu C, Kolb H. 1998. Interleukin-18 treatment of NOD mice suppresses Th1 insulitis and diabetes. Diabetes 47 (Suppl. 1):A202, 782.

Seder RA, Paul WE. 1994. Acquisition of lymphokine-producing phenotype by $CD4^+$ T-cells. Ann Rev Immunol 12:635–673.

Shehadeh NN, La Rosa F, Lafferty KJ. 1993. Altered cytokine activity in adjuvant inhibition of autoimmune diabetes. Autoimmunity 6:291–300.

Springer TA. 1990. Adhesion receptors of the immune system. Nature 346:425–434.

Suarez-Pinzon W, Rajotte RV, Mosmann TR, Rabinovitch A. 1996. Both $CD4^+$ and $CD8^+$ T-cells in syngeneic islet grafts in NOD mice produce interferon-γ during β-cell destruction. Diabetes 45:1350–1357.

Takaori K, Inoue K, Nio Y, Aung T, Fukumoto M, Hashida T, Yasuhara M, Hori R, Tobe T. 1992. Basic study on immunologic effects of cyclosporine and FK506 for application to pancreatic transplantation. Transpl Proc 24:894–896.

Uchio E, Matsumoto T, Tanaka SI, Ohno S. 1999. Soluble intercellular adhesion molecule-1 (ICAM-1), CD4, CD8, and interleukin-2 receptor in patients with Behcet's disease and Vogt–Koyanagi–Harada's disease. Clin Exp Rheumatol 17:179–184.

Wahl SM, Allen JB, Ohura K, Chenoweth DE, Hand AR. 1991. Interferon-gamma inhibits inflammatory cell recruitment and the evolution of bacterial cell-wall-induced arthritis. J Immunol 146:95–100.

Yagi N, Yokono K, Amano K, Nagata M, Tsukamoto K, Hasegawa Y, Yoneda R, Okamoto N, Moriyama H, Miki M, Tominaga Y, Miyazaki J, Yagita H, Okumora K, Mizoguchi A, Miki A, Ide C, Maeda S, Kasuga M. 1995. Expression of intercellular adhesion molecule 1 on pancreatic B cells accelerates B cell destruction by cytotoxic T-cells in murine autoimmune diabetes. Diabetes 44:744–752.